



Effect of (Mo, W) substitution for Nb on glass forming ability and magnetic properties of Fe–Co-based bulk amorphous alloys fabricated by centrifugal casting

Ilker Kucuk^{a,*}, Muratahan Aykol^b, Orhan Uzun^c, Mehmet Yildirim^b, Mehmet Kabaer^a, Nagehan Duman^b, Fikret Yilmaz^c, Kadir Erturk^d, M. Vedat Akdeniz^b, Amdulla O. Mekhrabov^b

^a Physics Department, Faculty of Arts and Sciences, Uludag University, Gorukle Campus, 16059 Bursa, Turkey

^b Novel Alloys Design and Development Laboratory (NOVALAB), Department of Metallurgical and Materials Engineering, Middle East Technical University, 06531 Ankara, Turkey

^c Physics Department, Faculty of Arts and Sciences, Gaziosmanpasa University, 60250 Tokat, Turkey

^d Physics Department, Faculty of Arts and Sciences, Namik Kemal University, 59030 Tekirdag, Turkey

ARTICLE INFO

Article history:

Received 25 July 2010

Received in revised form 23 October 2010

Accepted 2 November 2010

Available online 10 November 2010

PACS:

75.50.Kj

81.05.Kf

64.70.pe

Keywords:

Bulk metallic glasses (BMGs)

Centrifugal casting

Magnetic materials

ABSTRACT

In this study, effects of simultaneous Mo and W substitution for Nb additions on the stability and magnetic properties of Fe–Co-based bulk metallic glass (BMG) alloys fabricated by centrifugal casting are investigated. The saturation magnetization (J_s) and coercivity (H_c) for the as-cast $\text{Fe}_{36}\text{Co}_{36}\text{B}_{19.2}\text{Si}_{4.8}\text{X}_4$ ($\text{X} = \text{Nb}$ or $\text{Mo}_{0.5}\text{W}_{0.5}$) BMG alloys and melt-spun $\text{Fe}_{36}\text{Co}_{36}\text{B}_{19.2}\text{Si}_{4.8}\text{Mo}_2\text{W}_2$ were in the range of 1.02–1.57 T and 11.13–1685 A/m, respectively. The $\text{Fe}_{36}\text{Co}_{36}\text{B}_{19.2}\text{Si}_{4.8}\text{X}_4$ ($\text{X} = \text{Nb}$ or $\text{Mo}_{0.5}\text{W}_{0.5}$) BMG alloys in the shape of wedge with the maximum thickness of 1.5–2 mm were obtained successfully by means of conventional centrifugal casting. Replacing Nb with $\text{Mo}_{0.5}\text{W}_{0.5}$ deteriorates magnetic properties in bulk form and reduces the GFA of the alloy due to promoting the precipitation of non-magnetic compounds, while it results in good soft magnetic properties in melt-spun ribbon form.

© 2010 Elsevier B.V. All rights reserved.

1. Introduction

Iron-based metallic glasses attract technological interest as they exhibit superior magnetic properties when compared to their crystalline counterparts. These unique properties make them attractive candidates for magnetic applications. Various Fe-based alloy systems have been investigated in order to improve thermal stability and soft magnetic properties in bulk or melt-spun ribbon forms [1–3]. Such amorphous alloys may find broader application fields when they are produced in bulk form via more conventional casting techniques, where critical cooling rates are less than 10^2 K/s [4]. This can only be achieved if the glass forming ability (GFA) of Fe-based alloys is improved further. The term GFA is used to define the relative ease with which an alloy melt can be transformed into a glass. There are several empirical criteria proposed in the literature which help evaluate the degree of GFA based on parameters.

Among those, the reduced glass transition temperature (T_{rg}) has been proved to be generally applicable to most of the alloy systems. Briefly, this criterion states that higher values of the dimensionless parameter $T_{rg} = T_g/T_l$ indicate higher GFA [5], where T_g and T_l are glass transition and liquidus temperatures, respectively. In addition, supercooled liquid region ΔT_x ; that is, the difference between T_x and T_g , can be utilized as a measure of GFA. According to this criterion, the higher the ΔT_x , the stronger the resistance to crystallization, which again implies a higher GFA [6].

Since 1995, a large number of Fe-based bulk metallic glasses (BMGs) which contain Fe–(Al, Ga)–(P, C, B, Si), Fe–(Mo, Co, Ga)–(P, C, B, Si), Fe–(Co, Ni)–(Zr, Nb, Hf, Ta, Mo, W)–B, Fe–(Nb, Ta)–(Mo, Cr)–C–B, Fe–Ni–P–B, and (Fe, Co)–Ln–B (Ln: lanthanide) [7] have been introduced. Very promising BMGs have also been developed in Fe–B–Si–Nb system recently [8]. Moreover, with the help of partial substitution of Co for Fe and subsequent entropic contribution to GFA, synthesis of rod-shaped BMGs with diameters up to 5 mm and good soft magnetic properties have been achieved [9]. In this paper, the effects of both (Mo, W) or Nb addition on the GFA and magnetic properties of the $\text{Fe}_{36}\text{Co}_{36}\text{B}_{19.2}\text{Si}_{4.8}\text{X}_4$ ($\text{X} = \text{Nb}$

* Corresponding author. Fax: +90 224 2941899.

E-mail address: ikucuk@uludag.edu.tr (I. Kucuk).

Table 1Thermal and magnetic properties of $\text{Fe}_{36}\text{Co}_{36}\text{B}_{19.2}\text{Si}_{4.8}\text{X}_4$ alloys.

X	T_g (K)	T_x (K)	ΔT_x (K)	T_m (K)	T_i (K)	T_{rg}	t_{\max} (mm)	J_s (T)	H_c (A/m)
Nb	817	856	39	1302	1359	0.601	2.0	1.02	19
$\text{Mo}_{0.5}\text{W}_{0.5}$	–	799	–	1303	1388	–	1.5	1.25	1685
$\text{Mo}_{0.5}\text{W}_{0.5}$ (melt-spun ribbon)	778	824	46	1335	1391	0.559	–	1.57	11.1

or $\text{Mo}_{0.5}\text{W}_{0.5}$) BMG alloy fabricated by centrifugal casting are investigated.

2. Experimental procedure

The Fe–Co-based ingots with nominal compositions were first homogenized by arc-melting the pure elements in Zr-gettered argon atmosphere for at least four times. The ingots were then cast from boron nitrate-coated alumina crucibles into pre-cooled rectangular copper moulds with cavity dimensions of $t \text{ mm} \times 16 \text{ mm} \times 70 \text{ mm}$, where t varies between 1 and 3 mm, in argon atmosphere via a Manfredi Multihertz Neutromag Digital centrifugal casting device. This device is designed for industrial dentistry and jewellery applications. Rapidly solidified $\text{Fe}_{36}\text{Co}_{36}\text{B}_{19.2}\text{Si}_{4.8}\text{Mo}_2\text{W}_2$ ribbon was prepared by the single roller melt-spinning technique. During rapid cooling, a stream of molten alloy with temperature 1423 K was ejected by pressured argon from 0.5 mm diameter orifice onto brass wheel rotating at 30 m/s circumferential velocity. Resulting ribbon was typically 3 m long, 0.5 cm wide and 25 μm thick.

The T_g , T_x , T_i and melting temperature T_m were measured with Setaram SET-SYS 16/18 differential scanning calorimetry (DSC) under flowing high purity argon gas with 15–20 mg samples at a ramp rate of 0.67 K/s. The ΔT_x and T_{rg} were calculated accordingly. X-ray diffraction (XRD) was conducted with Rigaku D/MAX 2200 by monochromatic $\text{CuK}\alpha$ radiation to evaluate whether the analyzed region of the specimen is amorphous or retains crystalline phases. Magnetic hysteresis measurements were conducted with an ADE Magnetics EV9 vibrating sample magnetometer (VSM) with maximum magnetic field strength of 1750 kA/m, real-time field control and dynamic gauss range capable of reaching a resolution of 0.08 A/m at low fields. Relative permeability (μ_r) at 50 Hz and 1 kHz was measured with an ac B – H analyzer operated under sinusoidal input voltage by using the wound toroidal core with a diameter of about 30 mm. Alloy densities were measured with Archimedeian principle.

3. Results and discussion

The DSC patterns exhibited by BMGs are given in Fig. 1a and related thermal parameters are listed in Table 1 with the maximum attainable thickness (t_{\max}) values. $\text{Fe}_{36}\text{Co}_{36}\text{B}_{19.2}\text{Si}_{4.8}\text{Nb}_4$ alloy produced by centrifugal casting undergoes glass transition at 817 K which is followed by a subsequent crystallization at 856 K. The corresponding ΔT_x is smaller than the one reported by Hirata et al. [10] while it is larger than an older report [11]. With substitution of $\text{Mo}_{0.5}\text{W}_{0.5}$ for Nb, T_x value is found to be reduced to 799 K. However, no significant change of slope is observed to distinguish T_g in bulk $\text{Fe}_{36}\text{Co}_{36}\text{B}_{19.2}\text{Si}_{4.8}\text{Mo}_2\text{W}_2$ alloy. Fig. 1b shows the DSC pattern obtained for rapidly solidified $\text{Fe}_{36}\text{Co}_{36}\text{B}_{19.2}\text{Si}_{4.8}\text{Mo}_2\text{W}_2$ ribbon where T_g and T_x are marked by arrows and the corresponding values are reported in Table 1. The data obtained by thermal analysis reveal that the Mo and W substitution to Nb reduces both T_g and T_x in melt spun ribbon and T_x in the BMG alloy.

The XRD patterns of the as-cast $\text{Fe}_{36}\text{Co}_{36}\text{B}_{19.2}\text{Si}_{4.8}\text{X}_4$ BMG alloys shown in Fig. 2a indicate for $\text{X}=\text{Nb}$ that the alloy is fully X-ray amorphous, while for $\text{X}=\text{Mo}_{0.5}\text{W}_{0.5}$ that the alloy is in a partially amorphous state. It can be depicted from XRD pattern of the multi-component ribbon (Fig. 2b) that the alloy is fully amorphous, as evidenced by the absence of diffraction peaks.

The J – H loops for the as-cast $\text{Fe}_{36}\text{Co}_{36}\text{B}_{19.2}\text{Si}_{4.8}\text{X}_4$ BMG alloys and $\text{Fe}_{36}\text{Co}_{36}\text{B}_{19.2}\text{Si}_{4.8}\text{Mo}_2\text{W}_2$ ribbon are shown in Fig. 3. The J values have been calculated using the data of density and magnetization (M) for each measurement. J values of alloys are in the range 1.02–1.57 T. The saturation magnetization (J_s) and coercivity (H_c) of the ribbon and the as-cast BMGs are compared in Table 1. The simultaneous substitution of Mo and W for Nb increases J_s from 1.02 T to 1.25 T. Such an increase in J_s of $\text{Fe}_{36}\text{Co}_{36}\text{B}_{19.2}\text{Si}_{4.8}\text{Mo}_2\text{W}_2$

partially bulk glassy alloy can be explained by the precipitation of a constituent ferromagnetic phase such as Fe(Co), which eventually alters the overall magnetic response of the alloy. The as-cast melt spun fully amorphous ribbon shows the high saturation magnetization of 1.57 T. Typical magnetically soft H_c values were obtained for $\text{Fe}_{36}\text{Co}_{36}\text{B}_{19.2}\text{Si}_{4.8}\text{Nb}_4$ BMG alloy and $\text{Fe}_{36}\text{Co}_{36}\text{B}_{19.2}\text{Si}_{4.8}\text{Mo}_2\text{W}_2$ amorphous ribbon, while the partially amorphous $\text{Fe}_{36}\text{Co}_{36}\text{B}_{19.2}\text{Si}_{4.8}\text{Mo}_2\text{W}_2$ BMG alloy shows drastically increased coercivity. Similarly, comparing the coercivity of ribbon with the same bulk composition, a significant rise is observed. This can be attributed to the presence of non-magnetic crystalline phases co-precipitated with Fe(Co) phase, in agreement with the measured XRD patterns. Fig. 4 shows the variation of relative permeability with magnetic induction (B) for the melt spun

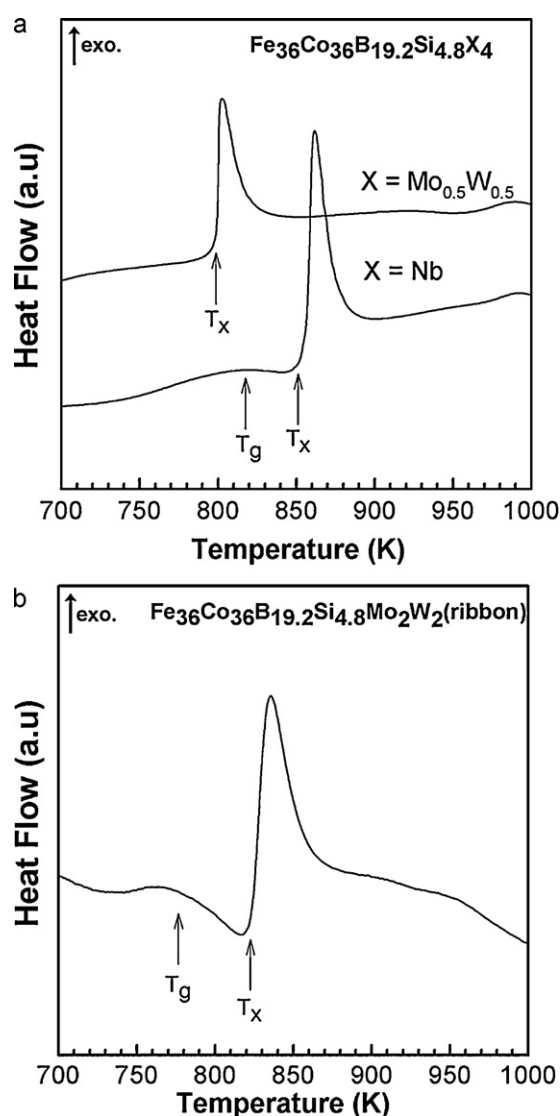


Fig. 1. (a) DSC patterns of $\text{Fe}_{36}\text{Co}_{36}\text{B}_{19.2}\text{Si}_{4.8}\text{X}_4$ BMG alloys with $\text{X}=\text{Nb}$ and $\text{X}=(\text{Mo}, \text{W})$ prepared by centrifugal casting and (b) DSC pattern of $\text{Fe}_{36}\text{Co}_{36}\text{B}_{19.2}\text{Si}_{4.8}\text{Mo}_2\text{W}_2$ melt spun ribbon.

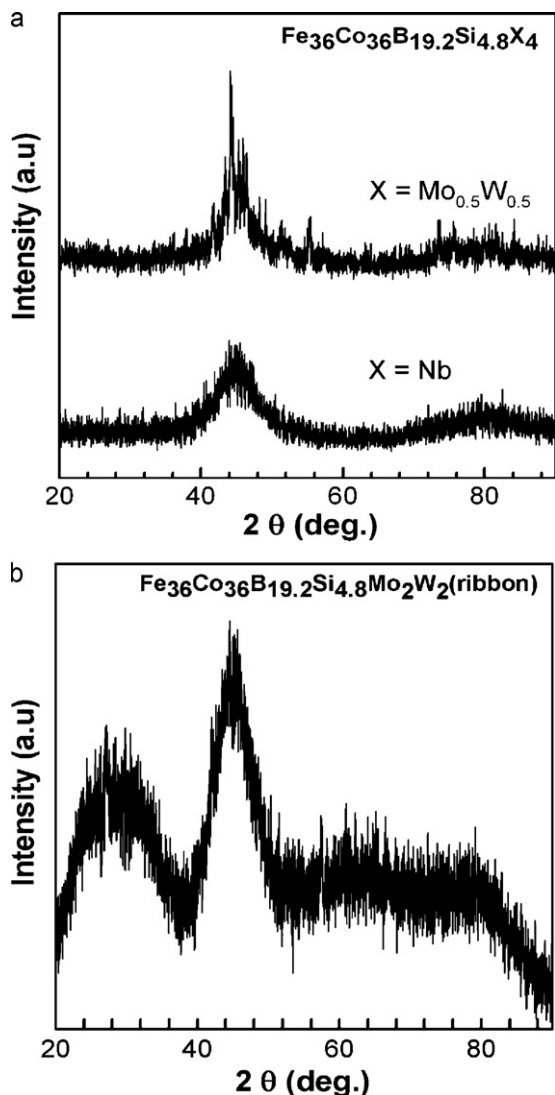


Fig. 2. XRD patterns of (a) the as-cast $\text{Fe}_{36}\text{Co}_{36}\text{B}_{19.2}\text{Si}_{4.8}\text{X}_4$ alloys with $\text{X} = \text{Nb}$ and $\text{X} = (\text{Mo}, \text{W})$ produced by centrifugal casting and (b) XRD pattern of $\text{Fe}_{36}\text{Co}_{36}\text{B}_{19.2}\text{Si}_{4.8}\text{Mo}_2\text{W}_2$ melt spun ribbon.

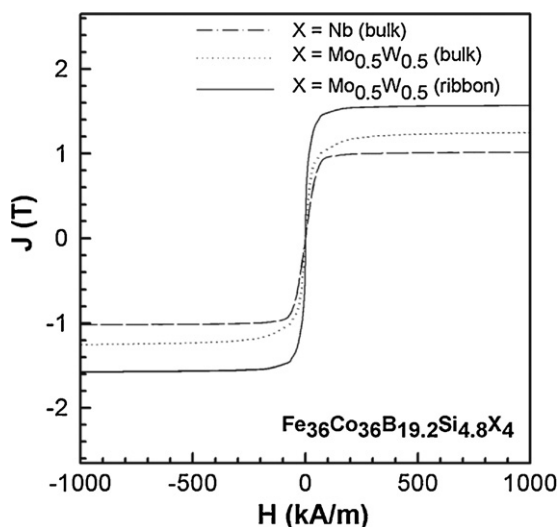


Fig. 3. Hysteresis loops of the as-cast $\text{Fe}_{36}\text{Co}_{36}\text{B}_{19.2}\text{Si}_{4.8}\text{X}_4$ BMG alloys with $\text{X} = \text{Nb}$ and $\text{X} = (\text{Mo}, \text{W})$, and $\text{Fe}_{36}\text{Co}_{36}\text{B}_{19.2}\text{Si}_{4.8}\text{Mo}_2\text{W}_2$ melt spun amorphous ribbon.

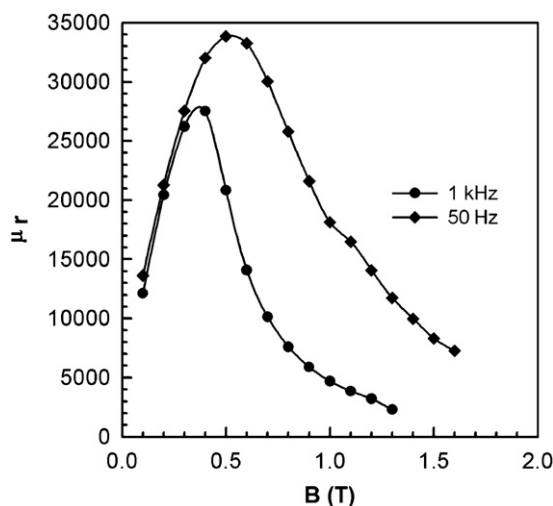


Fig. 4. The variation of relative permeability with magnetic induction in the rapidly solidified $\text{Fe}_{36}\text{Co}_{36}\text{B}_{19.2}\text{Si}_{4.8}\text{Mo}_2\text{W}_2$ ribbon.

$\text{Fe}_{36}\text{Co}_{36}\text{B}_{19.2}\text{Si}_{4.8}\text{Mo}_2\text{W}_2$ alloy. The maximum μ_r values have been approximately found to be 34,000 and 28,000 at 50 Hz and 1 kHz, respectively.

The results show that $\text{Fe}_{36}\text{Co}_{36}\text{B}_{19.2}\text{Si}_{4.8}\text{Nb}_4$ BMG alloy and $\text{Fe}_{36}\text{Co}_{36}\text{B}_{19.2}\text{Si}_{4.8}\text{Mo}_2\text{W}_2$ melt spun ribbon have good thermal and soft magnetic properties, while the presence of the precipitated phases in partially amorphous $\text{Fe}_{36}\text{Co}_{36}\text{B}_{19.2}\text{Si}_{4.8}\text{Mo}_2\text{W}_2$ bulk alloy provided increased saturation magnetization along with increased coercivity. Due to the higher cooling rates assured in the ribbon preparation, the $\text{Fe}_{36}\text{Co}_{36}\text{B}_{19.2}\text{Si}_{4.8}\text{Mo}_2\text{W}_2$ melt spun ribbon exhibits good magnetic softness; namely, H_c of 11 A/m and μ_r of 28,000 at 1 kHz and 0.4 T. However, the magnetic properties of such alloys prepared in bulk form are more important owing to their development in a totally conventional and simple route via centrifugal casting.

The main purpose of the (Mo, W) substitution to Nb was to investigate influence of such a substitution on GFA and subsequent magnetic properties of the alloy. Because simultaneous Mo and W addition increases the number of components of the system (thus one expects an entropic contribution to GFA and they are mostly used in such a way since they are elements with similar atomic radii) and they have been widely employed in several Fe-based BMGs as in Fe–Co–(Zr, Nb)–(Mo, W)–B type alloys [7]. However, it is found that such a substitution deteriorates the GFA and a fully amorphous form cannot be achieved in centrifugal casting but only via melt spinning in $\text{Fe}_{36}\text{Co}_{36}\text{B}_{19.2}\text{Si}_{4.8}\text{X}_4$ type alloys.

4. Conclusion

The effect of replacing Nb with (Mo, W) on glass formation and magnetic properties of the Fe–Co-based bulk metallic glasses has been examined. Fully and partially amorphous $\text{Fe}_{36}\text{Co}_{36}\text{B}_{19.2}\text{Si}_{4.8}\text{X}_4$ alloys with critical dimensions of 2 mm and 1.5 mm were obtained, respectively for $\text{X} = \text{Nb}$ and $\text{X} = \text{Mo}_{0.5}\text{W}_{0.5}$ additions by conventional centrifugal casting. We showed that such a substitution of $\text{Mo}_{0.5}\text{W}_{0.5}$ for Nb neither increases glass forming ability, nor improves magnetic softness because it promotes precipitation of undesired non-magnetic domain pinning phases which brings about drastic increases in coercivity. Magnetic measurements indicate a soft magnetic behavior for $\text{Fe}_{36}\text{Co}_{36}\text{B}_{19.2}\text{Si}_{4.8}\text{Nb}_4$ bulk metallic glass, while such a behavior is observed only in ribbon form for $\text{Fe}_{36}\text{Co}_{36}\text{B}_{19.2}\text{Si}_{4.8}\text{Mo}_2\text{W}_2$ alloy.

Acknowledgment

This work was supported by The Commission of Scientific Research projects of Uludag University, Project number UAP(F)-2010/19.

References

- [1] A. Inoue, X.M. Wang, W. Zhang, *Rev. Adv. Mater. Sci.* 18 (2008) 1–9.
- [2] R. Li, S. Kumar, S. Ram, M. Stoica, S. Roth, J. Eckert, *J. Phys. D: Appl. Phys.* 42 (2009) 1–6.
- [3] H.W. Chang, Y.C. Huang, C.W. Chang, C.C. Hsieh, W.C. Chang, *J. Alloy Compd.* 472 (2009) 166–170.
- [4] A. Inoue, *Acta Mater.* 48 (2000) 279–306.
- [5] H.A. Davies, in: F.E. Luborsky (Ed.), *Amorphous Metallic Alloys*, Butterworth and Co. (Publishers) Ltd., Great Britain, 1983, p. 8.
- [6] A. Inoue, *Bulk Amorphous Alloys: Preparation and Fundamental Characteristics*, Materials Science Foundations 4, Trans Tech Publications Ltd., Switzerland, 1998.
- [7] W.H. Wang, C. Dong, C.H. Shek, *Mater. Sci. Eng.* 44 (2004) 45–89.
- [8] A. Inoue, B. Shen, *Mater. Sci. Eng. A* 375–377 (2004) 302–306.
- [9] A. Inoue, B. Shen, C.T. Chang, *Acta Mater.* 52 (2004) 4093–4099.
- [10] A. Hirata, Y. Hirotsu, K. Amiya, N. Nishiyama, A. Inoue, *Intermetallics* 16 (2008) 491–497.
- [11] N.A. Mariano, C.A.C. Souza, J.E. May, S.E. Kuri, *Mater. Sci. Eng. A* 354 (2003) 1–5.